











Enhanced breast cancer cell targeting: RGD integrin ligand potentiates RWQWRWQWR's cytotoxicity and inhibits migration

Andrea Barragán-Cárdenas¹, Daniel Castellar-Almonacid², Yerly Vargas-Casanova³, Claudia Parra-Giraldo³, Adriana Umaña-Pérez⁴, Joel López-Meza⁵, Zuly Rivera-Monroy⁴, Javier García-Castañeda^{2*}

¹Instituto de Biotecnología, Universidad Nacional de Colombia, Bogotá 111321, Colombia

²Departamento de Farmacia, Universidad Nacional de Colombia, Bogotá 111321, Colombia

³Department of Microbiology, Faculty of Sciences, Pontificia Universidad Javeriana, Bogotá 110231, Colombia

⁴Departamento de Química, Universidad Nacional de Colombia, Bogotá 111321, Colombia

⁵Centro Multidisciplinario de Estudios en Biotecnología - Universidad Michoacana de San Nicolás de Hidalgo, Morelia 58030, México

***Correspondence:** Javier García-Castañeda, Departamento de Farmacia, Universidad Nacional de Colombia, Bogotá 111321, Colombia. jaegarciaca@unal.edu.co

Academic Editor: Fernando Albericio, Universities of KwaZulu-Natal, South Africa, Universidad de Barcelona, Spain

Received: May 2, 2024 **Accepted:** June 21, 2024 **Published:** July 19, 2024

Cite this article: Barragán-Cárdenas A, Castellar-Almonacid D, Vargas-Casanova Y, Parra-Giraldo C, Umaña-Pérez A, López-Meza J, et al. Enhanced breast cancer cell targeting: RGD integrin ligand potentiates RWQWRWQWR's cytotoxicity and inhibits migration. *Explor Drug Sci.* 2024;2:369–88. <https://doi.org/10.37349/eds.2024.00052>

Abstract

Aim: Evaluate the selective cytotoxic effect of the palindromic sequence RWQWRWQWR and its analogues obtained by replacement of L-amino acids by D-amino acids or the functionalization by adding the RGD (integrin ligand motif) to the peptide.

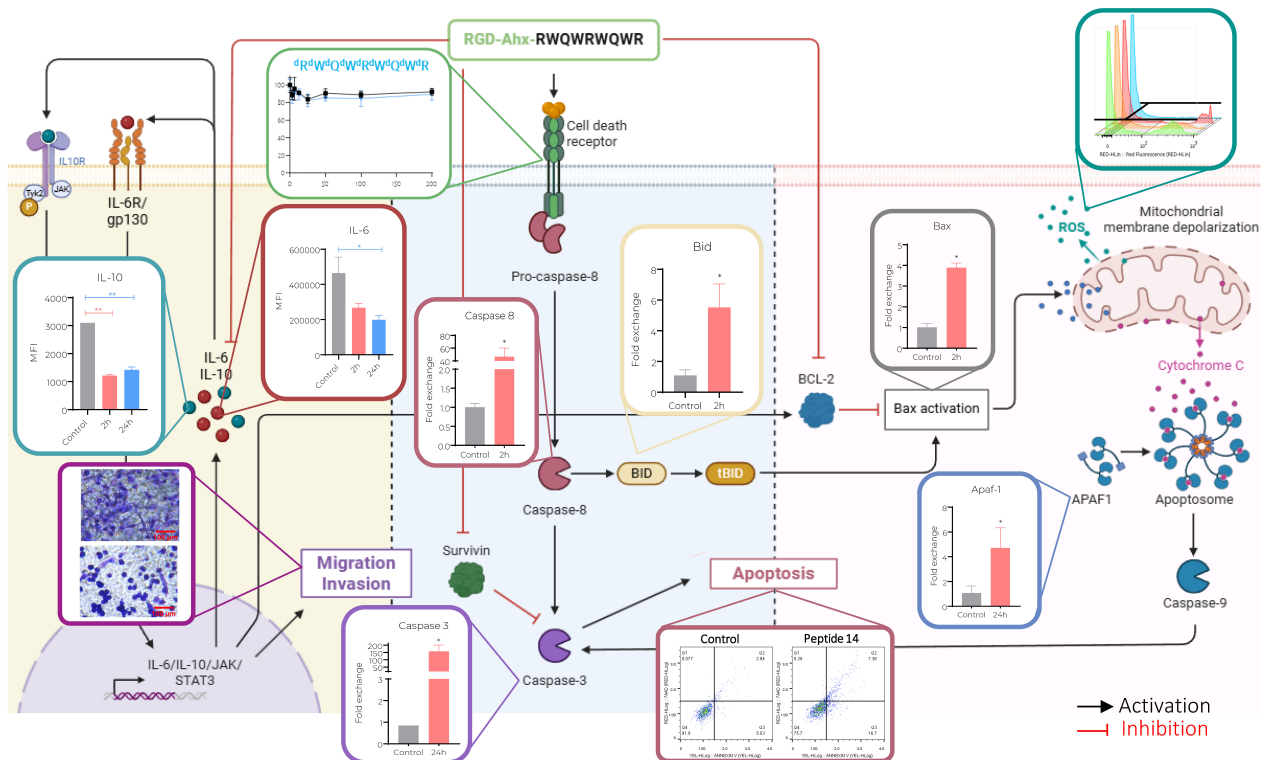
Methods: Peptides were obtained by SPPS, characterized by RP-HPLC and ESI-QTOF and its biological activity was evaluated using MTT assays. Evaluation of mechanism associated to the cytotoxic effect were carried out by flow cytometry, RT-qPCR, wound healing, transwell and zymography.

Results: The peptides with replacements of D-amino acid showed a lesser cytotoxic effect against breast cancer cell lines, regardless it was one or several residues modified which suggested a possible specific interaction between the peptide and the cancer cell membrane besides its initial electrostatically contact. On the other hand, addition of the RGD sequence to the palindromic peptide in the N-terminal end resulted in a greater cytotoxic effect against cell lines derived from the three mainly diagnosed breast cancer molecular subtypes. An approximation on mechanisms associated to this effect was evaluated on MCF-7 cells, it shows that the peptide induced apoptosis by activating intrinsic and extrinsic pathway, which correlates with the possibility of a specific interaction, and induces mitochondrial depolarization with release of oxygen reactive species. Also, this peptide induces a reduction in migration and invasion associated with a diminish in metalloprotease 9 activity and a lesser release of IL-6, IL-10 and arginase cytokines.

Conclusions: Our results suggest that this promising peptide can be considered for preclinical evaluation in the development of drugs to treat breast cancer and thus mitigate the impact of this disease.

© The Author(s) 2024. This is an Open Access article licensed under a Creative Commons Attribution 4.0 International License (<https://creativecommons.org/licenses/by/4.0/>), which permits unrestricted use, sharing, adaptation, distribution and reproduction in any medium or format, for any purpose, even commercially, as long as you give appropriate credit to the original author(s) and the source, provide a link to the Creative Commons license, and indicate if changes were made.





Graphical abstract. Proposed mechanism of action of peptide 14 (RGD-Ahx-RWQWRWQWR) in MCF-7 cells. Created by BioRender.com

Keywords

Breast cancer, anticancer peptides, apoptosis, migration

Introduction

Despite all efforts to reduce breast cancer incidence and mortality worldwide in the past few decades, to 2022 is still the second most diagnosed cancer with 2,308,931 new cases reported and, the fourth deadliest cancer with 669,418 deaths registered [1]. Breast cancer is a heterogenous disease that encompasses dissimilar clinical presentations, trajectories, and outcomes; this cancer is grouped in four intrinsic subtypes (luminal A, luminal B, HER2-enriched, and basal-like) mainly differentiated by the expression of membrane receptors among other 50 genes used in this classification; nowadays, typification is key to determine the therapeutic approach to each case [2].

Luminal A tumours are the most common, approximately 40% of diagnoses are typified in this category, they have genetic expression of oestrogen receptor (ER), progesterone receptor (PR), and lack of significant expression of human epidermal growth factor receptor 2 (HER2). Luminal B is the second most diagnosed subtype, accounting for more than 20% of new cases, these tumours are also ER+ and PR+ but have a higher expression of HER2, cell-cycle and proliferative related genes. The third most frequent subtype is basal-like, 15 to 20% of breast malignancies belong to this group characterized by the absence of ER, PR and HER2, with high expression of proliferation and cell adhesion genes [3, 4].

Although different therapeutic approaches are needed for each subtype, most patients are treated with systemic therapies to induce cell death and reduce tumour size, either as neoadjuvant or adjuvant therapy. These treatments have a major drawback which is the fact that they lack the selectivity required to only affect cancer cells inducing deleterious outcomes on non-cancerous cells and therefore side effects on patients like fatigue, alopecia, cytopenia, fibromyalgia, neurocognitive dysfunction, cardiomyopathy, second cancers, early menopause, and psychosocial affections among others [5, 6].

Peptides are a promising option for developing new treatments against breast cancer. Anti-cancer peptides (ACPs) are more selective for cancer cells, offer greater options for drug delivery, versatility in the suitability of the dosage form, have a broad spectrum of action and may induce fewer adverse effects. Some ACPs exert their effect through several pathways, which makes them less likely to induce resistance [7, 8]. Another great advantage is their ease of synthesis since they can be obtained with high purity and are therefore considered innocuous molecules. They also allow versatility in the optimization process, since the existing synthetic methods let them be modified in specific sites of the sequence, change of L-amino acids to D-amino acids, functionalization with peptides, proteins, carbohydrates, lipids, etc.

Lactoferricin B (LfcinB) is a 25 amino acid peptide derived from bovine lactoferrin, which have had activity against different types of cancer such as colorectal, oral, breast, cervix, lung, and leukaemia [9]. The six amino acid sequence RRWQWR is known as the minimal activity motif, and short peptides derived from it have shown higher activity than LfcinB [10]. The palindromic sequence RWQWRWQWR and its analog RRWQWRWQWR have shown lower IC₅₀ than the minimal motif and the LfcinB against MCF-7 and MDA-MB-231 breast cancer cell lines with minimum cytotoxic effect on red blood cells, fibroblast and MCF-12 cells [11].

To improve the anticancer activity of the palindromic peptide, two approaches were carried out: the first one consisted in changing totally or partially the L-amino acids by D-amino acids (Table 1). This approach seeks to maintain the cytotoxic effect against cancer cells and increase resistance to proteolytic degradation. The following changes were made: Each L-amino acid was changed by the respective D-amino acid, all L-Trp were changed by D-Trp, all L-Arg by D-Arg, all L-Gln by D-Gln and all L-amino acids of the sequence were changed by D-amino acids.

Table 1. Peptides derived from RWQWRWQWR (¹R⁵R⁹R) sequence containing D-aminoacids. Characterization by RP-HPLC and ESI-QTOF MS, and cytotoxic effect against breast cancer cells and non-cancerous fibroblast primary cell culture

Code	Sequence	RP-HPLC		ESI-MS (M ^a)		IC ₅₀ , µg/mL (µM)	
		t _R (min)	Purity (%)	Theoretical	Exp.	MCF-7	Fibroblasts
¹ R ⁵ R ⁹ R	RWQWRWQWR	6.3	92	1,485.75	1,485.88	120 (81)	> 200 (135)*
1	^d RWQWRWQWR	5.9	99	1,485.76	1,485.77	> 200 (135)*	> 200 (135)*
2	R ^d WQWRWQWR	6.7	94	1,485.76	1,485.77	> 200 (135)*	> 200 (135)*
3	RW ^d QWRWQWR	5.9	99	1,485.76	1,485.76	> 200 (135)*	> 200 (135)*
4	RWQ ^d WRWQWR	6.5	95	1,485.76	1,485.77	> 200 (135)*	> 200 (135)*
5	RWQW ^d RWQWR	5.9	95	1,485.76	1,485.77	> 200 (135)*	> 200 (135)*
6	RWQWR ^d WQWR	6.1	89	1,485.76	1,485.77	> 200 (135)*	> 200 (135)*
7	RWQWRW ^d QWR	6.1	100	1,485.76	1,485.77	> 200 (135)*	> 200 (135)*
8	RWQWRWQ ^d WR	6.3	98	1,485.76	1,485.77	> 200 (135)*	> 200 (135)*
9	RWQWRWQW ^d R	6.3	99	1,485.76	1,485.77	> 200 (135)*	> 200 (135)*
10	^d RWQW ^d RWQW ^d R	5.4	94	1,485.76	1,485.77	> 200 (135)*	> 200 (135)*
11	R ^d WQ ^d WR ^d WQ ^d WR	6.5	99	1,485.76	1,485.77	> 200 (135)*	> 200 (135)*
12	RW ^d QWRW ^d QWR	5.6	99	1,485.76	1,485.77	> 200 (135)*	> 200 (135)*
13	^d R ^d W ^d Q ^d W ^d R ^d W ^d Q ^d W ^d R	6.4	90	1,485.76	1,485.77	> 200 (135)*	> 200 (135)*

^dR, ^dW, ^dQ indicate the position of D-Arg, D-Trp and D-Gln, respectively. *: IC₅₀ could not be reached at the evaluated concentrations; ESI-MS: electrospray ionization mass spectrometry; IC₅₀: half maximal inhibitory concentration; M^a: corresponds to monoisotopic mass; RP-HPLC: reversed-phase high-performance liquid chromatography; t_R: retention time

The second approach was to incorporate the RGD or DGR sequence to increase the cytotoxic effect and selectivity for breast cancer cells. This tripeptide has been used as a radiotracer to target breast cancer cells due to its affinity to the integrin αvβ3, usually overexpressed in this kind of tumours [12]. We explored the effect of the addition of the sequence in the C, N-terminal or both against MCF-7, BT-474, MDA-MB-231 and MDA-MB-468 cells belonging to the three most diagnosed subtypes of molecular breast cancer. Functionalization on the N-terminal exert cytotoxic activity against all cell types evaluated, being MCF-7

cells the most affected by it. In these luminal A cells, the functionalized peptide RGD-Ahx-RWQWRWQWR induced apoptosis with release of reactive oxygen species along with the diminish of invasiveness and migration of cells.

Materials and methods

Fmoc/tBu solid phase peptide synthesis

Briefly, 200 mg of Merck's rink amida resin (0.046 mEq/g) was swollen and solvated as stipulated by the manufacturer. The resin was then treated with piperidine solution (5% in DMF), twice, to get the free amine group. Then the coupling of the first amino acid from the C-terminal end of the sequence was carried out, and the formation of the peptide bond was confirmed by Kaiser test. These deprotection and coupling processes were repeated until the peptide sequence was completed. Finally, the peptide was cleaved from the resin and the side chains were deprotected using a cocktail that contained TFA, water and TIS.

Purification by solid phase extraction

Supelclean™ LC-18 SPE solid phase extraction columns of 5 g were activated with 30 mL of methanol, 30 mL of Solvent B (TFA 0.05 % in ACN) and equilibrated with 30 mL Solvent A (TFA 0.05 % in water). The peptide dissolved in Solvent A (150 mg/mL) was seeded on the column and eluted by a step gradient with increasing concentrations of Solvent B, the fractions were collected and analyzed by RP-HPLC, then the fractions with higher chromatographic purity were pooled and lyophilized [13].

Analysis by mass spectrometry

Peptides (10 µg/mL) were analyzed on a Bruker Impact II LC Q-TOF MS spectrometer equipped with an ESI ionization source operated in positive mode. The chromatographic conditions were Intensity Solo C18 column (2.1 × 100 mm, 1.8 µm, Bruker), at a temperature of 40°C and a flow of 0.250 mL/min. Solvent A [H₂O-Formic acid (FA) 0.1%], Solvent B (ACN-FA 0.1%). Elution gradient 5/5/95/95/5/5% Solvent B in 0/1/11/13/13.1/15 min. The ESI source conditions were: ionization energy 500 V, capillary 4,500 V, nebulizer 1.8 bar, dry nitrogen gas 8.0 L/min, temperature 220°C. Auto MS/MS scanning mode with spectral range 20–1,000 *m/z* and spectral rate 2 Hz and collision energy of 5.0 eV.

Cytotoxic effect in vitro

The cytotoxic effect of the peptides was evaluated depending on the stage against 4 lines derived from breast cancer, each belonging to a molecular subtype, or 1 mammary epithelial cell line and 1 primary fibroblast culture; to determine the selectivity of each peptide. Each peptide was evaluated in triplicate at times of 2, 24, and 48 h of incubation and concentrations of 6.25, 12.5, 25, 50, 100 and 200 µg/mL. Once the time had elapsed, 10 µL of MTT was added to each well and incubated for 4 h, then the medium was removed, 100 µL of sterile DMSO was added and incubated for 40 min at 37°C to solubilize the crystals of formazan and read absorbance at 570 nm. Based on the cell viability results, the peptide with the highest cytotoxicity and selectivity was selected to carry out the preliminary study of the mechanism of action. Three technical replicates were carried out.

Primary culture of human fibroblasts was isolated from foreskin in the Cellular and Molecular Physiology Laboratory of the Department of Medicine of the Universidad Nacional de Colombia.

The cell lines MDA-MB-468 (basal A triple-negative breast adenocarcinoma cell line), MDA-MB-231 (basal B triple-negative breast adenocarcinoma cell line), MCF-7 (metastatic breast adenocarcinoma cell line type luminal A), and BT-474 (ductal carcinoma cell line invasive luminal B) were used as models of each of the most prevalent molecular subtypes of breast cancer.

Hemolysis

Blood obtained from a healthy volunteer, peripheral blood was extracted by venipuncture, centrifuged at 800 *g* for 15 min at 10°C, and washed three times with 0.9% saline solution. A sample of red blood cells with a 4% hematocrit was prepared in saline solution. In a 96-well U-shaped box, 100 µL per well was

transferred and 100 μ L of the reconstituted peptide in 0.9% saline solution was added (400, 200, 100, 50 and 25 μ g/mL); each peptide was evaluated in triplicate at an incubation time of 2 h at 37°C. After the time, the box was centrifuged at 800 g for 5 min, 100 μ L of supernatant was transferred to a flat-bottomed 96-well box and absorbance was read at 540 nm. Saline solution (0.9%) was used as a negative control and Tween 20 was used as a positive control. Three technical replicates were carried out. The percentage of hemolysis was calculated according to the following equation:

$$\text{Hemolysis \%} = \frac{\text{ABS treatment} - \text{ABS negative control}}{\text{ABS positive control} - \text{ABS negative control}} \times 100$$

Apoptosis/necrosis assessment

MCF-7 cells were seeded in 24-well dishes at a rate of 15×10^4 cells/well and treated with peptide reconstituted in not supplemented medium for a final concentration of the IC_{50} . Cells were harvested and transferred to 2 mL conical centrifuge tubes, centrifuged at 300 g for 5 min, the supernatant was discarded and resuspended in 400 μ L of staining buffer solution with the fluorochromes of Millipore Muse™ Annexin V & Dead Cell Kit (1X annexin V binding buffer, 0.5 μ L of FITC annexin V and 0.5 μ L of 7-AAD per 5×10^6 cells). The cells with the fluorochromes were incubated in the dark for 15 min at 37°C, then centrifuged at 300 g for 10 min, resuspended in 200 μ L of 1 mM PBS and analyzed by flow cytometry in the Guava® Muse® Cell Analyzer. As an apoptosis control, the cells were treated with 4% formaldehyde and as negative control cells without treatment [14]. Cell-based experiments were repeated in two independent experiments performed in technical triplicates ($n = 3$).

Assessment of mitochondrial permeability

The cells were seeded in 24-well dishes at a rate of 15×10^4 cells/well, once adhered the culture medium was replaced with 200 μ L of the medium supplemented with 10% FBS plus 200 μ L of the peptide reconstituted in not supplemented medium, for a final concentration of IC_{50} . They were washed with PBS and stained with 100 μ L of the working solution of the BD Pharmingen™ MitoScreen JC-1 commercial kit (1:100 solution of JC1 reconstituted in DMSO: buffer assay 1X) for 20 min at 37°C. They were then washed twice with the assay buffer provided in the kit and resuspended in 100 μ L of this for reading in the BD Accuri™ C6 cytometer, detecting the emission of the monomeric form at 527 nm and that of the aggregates at 590 nm. Negative control: labeled untreated cells, positive control: cells treated with actinomycin 10 μ g/mL for 24 h or 4% formaldehyde [14]. Cell-based experiments were repeated in two independent experiments performed in technical triplicates ($n = 3$).

Evaluation of reactive oxygen species

The cells were cultured and treated as in the previous item. After 2 and 24 h of treatment, the medium was removed, the cells were harvested, transferred to a microcentrifuge tube and resuspended in assay buffer at a rate of 1×10^6 cells/mL. Of this suspension, 10 μ L was transferred to a tube. Microcentrifuge and 190 μ L of Muse® Oxidative Stress working solution was added, it was incubated at 37°C for 30 min and reading was performed on the Guava Muse® cytometer. The assay was performed in biological duplicate, as a negative control: labeled untreated cells and as a positive control: cells treated with 4% formaldehyde [15]. Cell-based experiments were repeated in two independent experiments performed in technical triplicates ($n = 3$).

Evaluation of cytokine secretion

The cells were cultured, harvested and treated as in the previous item. After 2 and 24 h of treatment, the supernatants were recovered and stored at -20°C until analysis. In 1.5 mL tubes, 25 μ L of assay buffer, 25 μ L of supernatant from each treatment and 25 μ L of the bead premix included in the LEGENDplex™ Human Macrophage/Microglia Panel kit were added, incubated in the dark for 2 h, centrifuged at 1,050 rpm, then the supernatant was removed, and the pellet was washed with washing buffer. Detection antibodies (25 μ L) were added to the pellet and it was incubated for 1 h in the dark. Subsequently, 25 μ L of SA-PE was added and the incubation continued for an additional 30 min. After the time, it was centrifuged at 1,050 rpm, the

supernatant was removed, washed with washing buffer and resuspended in 150 μL of washing buffer. Cytometry analysis was performed on the Cytex Aurora device to determine the secretion of IL-12p70, TNF- α , IL-6, IL-4, IL-10, IL-1 β , arginase, TARC, IL-1RA, IL-12p40, IL-23, IFN- γ and IP-10 (B9). For this, use was made of the proposed template and software proposed in the LEGENDplex™ Human Macrophage/Microglia Panel kit [16]. Cell-based experiments were performed in technical duplicates ($n = 2$).

Wound-healing test

Cells at 70–80% confluency were subcultured in 24-well dishes at a rate of 3×10^5 cells/well, for 12 h until adherence. The medium was then removed and 100 μL of unsupplemented RPMI was added to synchronize the culture for 12 h. With the tip of a micropipette, the monolayer was broken vertically along the well, the unsupplemented medium was removed and medium with 5% SFB (negative control), medium with 20% SFB (positive control) or peptide at the concentrations of IC_{50} , 0.5 IC_{50} and 2 IC_{50} dissolved in medium with 5% SFB was added. In the microscope, 4 photographs were taken from different fields that allowed the entire length of the wound to be covered; and this process was repeated at 2, 12, 24 and 48 h of incubation, since it was made by triplicate twice, a total of 24 microphotographs per treatment were analyzed. Using ImageJ, the lesion area was calculated after the different time periods and compared with that at time 0 [17].

Migration test

Breast cancer-derived cells were cultured in the upper well of 12-well plates with 8 μm pore transwell at a density of 15×10^4 cells/well in 100 μL of serum-free medium. In the lower wells, the controls and treatments with the peptide (IC_{50}) were added in a final volume of 600 μL ; the transwell was placed over the lower well containing the stimulus and migration was allowed by incubating at 37°C for 2, 12 and 24 h. After time, the medium and stimuli were removed and 600 μL of 4% paraformaldehyde solution was added to the lower well for 15–30 min to allow the cells to fix on the membrane of the upper well. Paraformaldehyde was recovered and 600 μL of a 0.5% crystal violet solution in methanol was added to the lower well, staining for 15–30 min. The solution was removed and the transwells were washed with water and cotton swabs; 1 mL of water was added to the lower wells and 100 μL to the upper wells. Under the microscope, the cells in each well were counted and 5 microphotographs were taken per membrane for a total of 10 microphotographs related to each treatment and time evaluated. The membranes were removed and placed in a microcentrifuge tube where 100 μL of 10% acetic acid solution was added to dissolve the stain and determine the absorbance at 570 nm in a microplate reader. The percentage of cell migration for each well was determined by dividing the number of cells that were counted in the transwell by the initial number of cells seeded [18]. Cell-based experiments were performed in technical duplicates ($n = 2$).

Invasion test

Using pre-cooled material, 100 μL of a solution containing Geltrex® (Invitrogen), covering buffer and cell maintenance medium were deposited in each transwell, allowed to gel overnight at 37°C in an incubator and then the same assay process as migration previously described was carried out [18]. Cell-based experiments were performed in technical duplicates ($n = 2$).

Zymography

The cells derived from breast cancer were cultured in 24-well plates at a rate of 15×10^4 cells/well. Once adhered, the culture medium was replaced with 200 μL of the medium supplemented with 10% FBS plus 200 μL of the peptide reconstituted in medium without supplement for a final concentration of IC_{50} . After 2 and 24 h of treatment, the supernatants were recovered and stored at -20°C until analysis. Denaturing electrophoresis of the supernatants was performed with a 10% separation gel supplemented with 0.05% gelatin and a 4% concentrating gel at 25 mA for 2.5 h. Following this, the gel was washed three times with Triton™ X-100 3% and three times with distilled water. It was incubated in gelatinase activation buffer for 30 min at room temperature and for 14 h at 37°C. Subsequently, it was stained with Coomassie blue in

MeOH/acetic acid for 3 h, washed 3 times with hot water (40–70°C) for 10 min each and then with decolorizing solution of acetic acid, methanol, and water (1:3:6) until visualized. Cell-based experiments were performed in technical duplicates ($n = 2$).

***Galleria mellonella* in vivo assay**

Galleria mellonella larvae (supplied by Perkin SAS) were placed in sterile glass Petri dishes at a rate of 10 larvae per dish. The prolegs of the larva were cleaned with a swab and 70% hypochlorite, then 10 μ L of peptide were inoculated at concentration of 800 μ g/mL in 0.9% saline solution, in the last right proleg. The treatment group was made up of 10 larvae and 2 replicates were made. As a control, 10 uncleaned larvae were used, as an absolute control, 10 larvae that were cleaned were used, and as an inoculation control, 10 larvae were inoculated with 0.9% saline solution. The larvae were incubated at 37°C and monitored for 10 days. Viability data were analyzed using Kaplan Meyer curves. The protocol used was implemented by the Human Proteomics and Mycoses Laboratory, under the principles and standards of the ethics committee for the care and use of animals, decreed by the institutional ethics committee of the Pontificia Universidad Javeriana.

Statistical analysis

Using the GraphPad Prism 4 program, comparisons within a treatment group were made using a one-way ANOVA or between treatments using two-way ANOVA, followed by Tukey's multiple comparisons test. Differences are considered significant at $p < 0.05$.

Results

Peptide synthesis

Peptides were synthesized by SPPS-Fmoc/tBu, purified and characterized by RP-HPLC and ESI-QTOF MS. The synthesis of the palindromic peptide ($^1R^5R^9R$) and its analogs (peptides 1 to 13) presented no difficulties and was similar to that of the original palindromic peptide. All peptides showed high purity (between 89–100%) and the expected mass corresponded to the theoretical mass in all cases. Chromatographic profiles showed that diastereomer peptides 2, 4, 11 and 13 had higher t_R (retention time) than the original palindromic peptide, while peptides 1, 3, 5–7, 10 and 12 had lower t_R , suggesting that some diastereomer peptides interact to a greater or lesser extent with the stationary phase even though they all have the same number of positively charged (Arg), hydrophobic (Trp) and polar uncharged (Gln) amino acids. When L-Arg was changed by D-Arg, peptides 1 and 5 showed similar t_R and lesser than peptides 9 and 13, suggesting that the change of L-Arg by D-Arg in position nine or in all positions of the sequence induced conformational changes that affect the interaction with stationary phase.

The tripeptide RGD and/or DGR was added either on the N-terminal end, on the C-terminal end or in both ends, of the $^1R^5R^9R$ and the $R^1R^5R^9R$ peptides. All synthetic processes were viable, peptides with purities greater than 90% were obtained and the experimental masses corresponded to the expected mass values of each peptide, in all cases (Table 2). When comparing with the synthetic processes of the $^1R^5R^9R$ it was evident that the addition of the RGD or DGR motif to the sequence did not affect it and that the inclusion at the N or C-terminus did not induce changes in the t_R of the molecules, indicating that the polarity was not significantly affected.

Cytotoxic effect against breast cancer cell lines

Effect of all peptides including the original sequences $^1R^5R^9R$ and $R^1R^5R^9R$ were evaluated against breast cancer derived cell line MCF-7 and, primary cell culture of fibroblast and red blood cells to assess the selectivity of each peptide. The results show that neither the diastereoisomers nor enantiomer exert the same or greater cytotoxicity against breast cancer cells MCF-7 meaning that the stereochemistry of the palindromic sequence is critical to its activity (Table 1).

Table 2. Peptides derived from RWQWRWQWR (¹R⁵R⁹R) sequence containing RGD or DGR motifs. Characterization by RP-HPLC and ESI-QTOF MS, and cytotoxic effect against breast cancer cells and non-cancerous fibroblast primary cell culture

Code	Sequence	RP-HPLC		ESI-MS (M)		IC ₅₀ , µg/mL (µM)	
		t _R (min)	Purity (%)	a	b	MCF-7	Fibroblasts
¹ R ⁵ R ⁹ R	RWQWRWQWR	6.3	92	1,485.75	1,485.88	120 (81)	> 200 (135)*
14	RGD-X-RWQWRWQWR	6.3	92	1,928.21	1,928.48	27 (14)	108 (56)
15	RWQWRWQWR-Ahx-RGD	6.3	96	1,928.21	1,928.46	> 200 (104)*	> 200 (104)*
16	RGD-X-RWQWRWQWR-X-RGD	6.1	84	2,369.69	2,368.99	> 200 (84)*	> 200 (84)*
17	DGR-X-RWQWRWQWR-X-RGD	6.0	99	2,369.69	2,369.67	> 200 (84)*	> 200 (84)*
18	DGR-X-RWQWRWQWR-X-DGR	6.1	95	2,369.69	2,369.80	> 200 (84)*	> 200 (84)*
R¹R⁵R⁹R	RRWQWRWQWR	6.2	93	1,631.87	1,641.88	112 (68)	> 200 (121)*
19	RGD-X-RRWQWRWQWR	6.2	95	2,084.39	2,084.62	82 (39)	195 (94)
20	RRWQWRWQWR-Ahx-RGD	6.2	98	2,084.39	2,084.62	> 200 (96)*	> 200 (96)*
21	RGD-X-RRWQWRWQWR-X-RGD	6.6	97	2,525.88	2,525.42	> 200 (79)*	> 200 (79)*
22	DGR-X-RRWQWRWQWR-X-RGD	6.2	95	2,525.88	2,525.95	> 200 (79)*	> 200 (79)*
23	DGR-X-RRWQWRWQWR-X-DGR	6.2	98	2,525.88	2,426.321	> 200 (79)*	> 200 (79)*

*: IC₅₀ could not be reached at the evaluated concentrations; a: theoretical; b: experimental monoisotopic mass in uma; ESI-MS: electrospray ionization mass spectrometry; IC₅₀: half maximal inhibitory concentration; RP-HPLC: reversed-phase high-performance liquid chromatography; t_R: retention time

Table 3. Cytotoxic and selective effect of RWQWRWQWR peptide and peptides functionalized with the RGD motif

Code	Peptide	IC ₅₀ , µg/mL (µM)		Selectivity index	Hemolysis (%) ^a
		MCF-7	Fibroblasts		
¹ R ⁵ R ⁹ R	RWQWRWQWR	120 (81)	> 200 (135)*	> 1.6	6.7
14	RGD-Ahx-RWQWRWQWR	27 (14)	108 (56)	4.0	7.1
R¹R⁵R⁹R	RRWQWRWQWR	112 (68)	> 200 (121)*	> 1.8	6.4
19	RGD-Ahx-RRWQWRWQWR	82 (39)	195 (94)	2.4	2.0

^a Percentage of hemolysis calculated at the maximum concentration (200 µg/mL). *: IC₅₀ could not be calculated because at the maximum concentration, there was no reduction in viability by 50%; IC₅₀: half maximal inhibitory concentration

Regarding the peptides containing the RGD motif, when it was added at the C-terminal end the analog peptides 15–18 and 20–23 did not present a significant cytotoxic effect, indicating that the incorporation of this motif at that end induced the loss of the cytotoxic activity of the sequence in MCF-7 cells, demonstrating that they are not viable as activity enhancers (Table 2). Contrary to this, when the RGD motif was added only at the N-terminal end, the cytotoxic effect against MCF-7 cells was significantly increased compared to its original peptide. Peptides 14 and 19 presented a significant lower IC₅₀ (14 and 39 µM respectively) compared to that of the ¹R⁵R⁹R or its analog sequence R¹R⁵R⁹R.

About selectivity, 14 and 19 peptides did not generate significant hemolysis in red blood cells, while in fibroblasts these peptides (IC₅₀ = 56 and 94 µM respectively) showed a cytotoxic effect greater than that evidenced by the non-functionalized sequences. However, when calculating the selectivity index, peptides 14 and 19 showed selectivity index higher than 1, which indicates that the peptide does discriminate normal cells from cancerous cells (Table 3).

Taking into consideration that peptide 14 is the sequence with the lowest IC₅₀ against MCF-7 and with the highest selectivity index, its cytotoxic activity was evaluated at times of 2, 24 and 48 h against cell lines derived from different molecular subtypes of breast cancer: MCF-7 (luminal A subtype), BT-474 (luminal B subtype), MDA-MB-468 (triple negative subtype A) and MDA-MB-231 (triple negative subtype B).

To compare the overall cytotoxic activity of the functionalized peptide 14 and the original palindromic sequence, the IC₃₀ values obtained for each time point and cell line evaluated are shown in Figure 1. This information allows us to determine that both peptides evaluated have a cytotoxic effect at short times, which does not vary significantly over time, being only dependent on the increase in concentration.

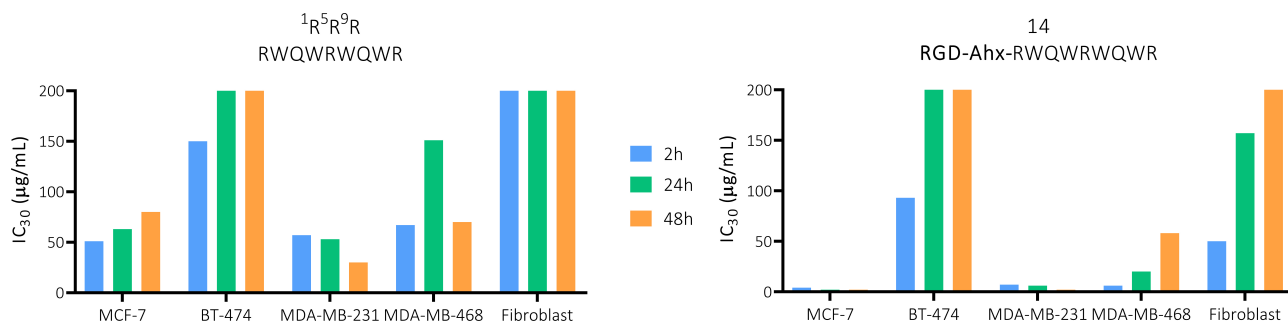


Figure 1. Effect on viability in MCF-7, BT-474, MDA-MB-231 and MDA-MB-468 breast cancer-derived cells, and primary fibroblast culture of the peptide palindromic peptide (RWQWRWQWR) and the 14 peptide (RGD-Ahx-RWQWRWQWR) at 2, 24 and 48 h of activity ($n = 3$)

BT-474 and MDA-MB-231 cell lines were less sensitive to the treatment of both peptides, so they did not generate a 50% decrease in cell viability. In these cases, functionalization with the tripeptide, although it maintained the cytotoxicity of the palindrome, did not significantly increase it. In MDA-MB-468 cells, an increase in the cytotoxic effect was evident compared to the palindrome, generating a cytotoxic effect at lower concentrations of the peptide with IC₅₀ of 22, 18 and 10 µM for 2, 24 and 48 h, respectively. Similarly, against MCF-7, the functionalized peptide exerted a greater cytotoxic effect with IC₅₀ of 14, 24 and 29 µM at 2, 24 and 48 h, respectively. Furthermore, there were no significant differences at the times evaluated, suggesting that the peptide exerts a rapid and long-lasting cytotoxic effect in both cell lines (Figure S1 and S2).

The primary culture of fibroblasts after 2 h of peptide activity denotes a decrease in cellular metabolism that reduces its viability nearly by 50%, however, after 24 h this effect on cellular metabolism is minor, since viability was close to 80%. Finally, 48 h after treatment with the peptide, the cells have recovered their normal activity, which means that the peptide may cause a temporary effect over cell metabolism that is overcome later by the cell regaining its normal function.

This information allows us to determine that both peptides evaluated have a cytotoxic effect at short times, which does not vary significantly over time, being only dependent on the increase in concentration. The functionalized peptide decreased the cell viability of all cell types evaluated at least at one time of activity. In all cases, this peptide decreased the IC₃₀ values, indicating that the addition of the RGD tripeptide increased the cytotoxic effect of the palindromic sequence.

Mechanisms associated with cytotoxic effects

Flow cytometric assays with annexin V/7-AAD were performed to establish the type of cell death induced in MCF-7. Cells were treated for 2 or 24 h with peptide 14 at the IC₅₀ concentration (14 µM). After 2 h of treatment, 43% of the cell population is alive and in the remaining 57% a significant cytotoxic effect of the peptide is observed (Figure 2C), which is mainly mediated by apoptotic events, evidencing an increase in labeling with annexin V (Figure 2B) that denotes a movement in the population towards quadrants Q2 and Q3 (Figure 2A). Of these events, 19% correspond to unique labeling with annexin V and, therefore, cells in early apoptosis. Thirty-seven percent of the events present double labeling with both annexin V and 7-AAD, establishing them as a population in late apoptosis; and only 1% of the population presented labeling with 7-AAD indicating necrosis because of the action of the peptide.

Similarly, when the cells were treated with the peptide 14 for 24 h, a significant decrease in the percentage of live cells significantly mediated by apoptotic events was also evident (Figure 2). In this case, 16% of the population was associated with early apoptotic events and 9% with late apoptotic events, indicating that the peptide exerts changes in the cells that allow for induction of apoptosis in the population after 24 h.

To confirm apoptotic events, the activation of caspases (Figure 3) and the depolarization of the mitochondrial membrane (Figure 4) were determined. In Figure 3 Panel A, the population that moves towards the Q1 quadrant is less than 1%, indicating, consistent with the test in Figure 2, that less than 1%

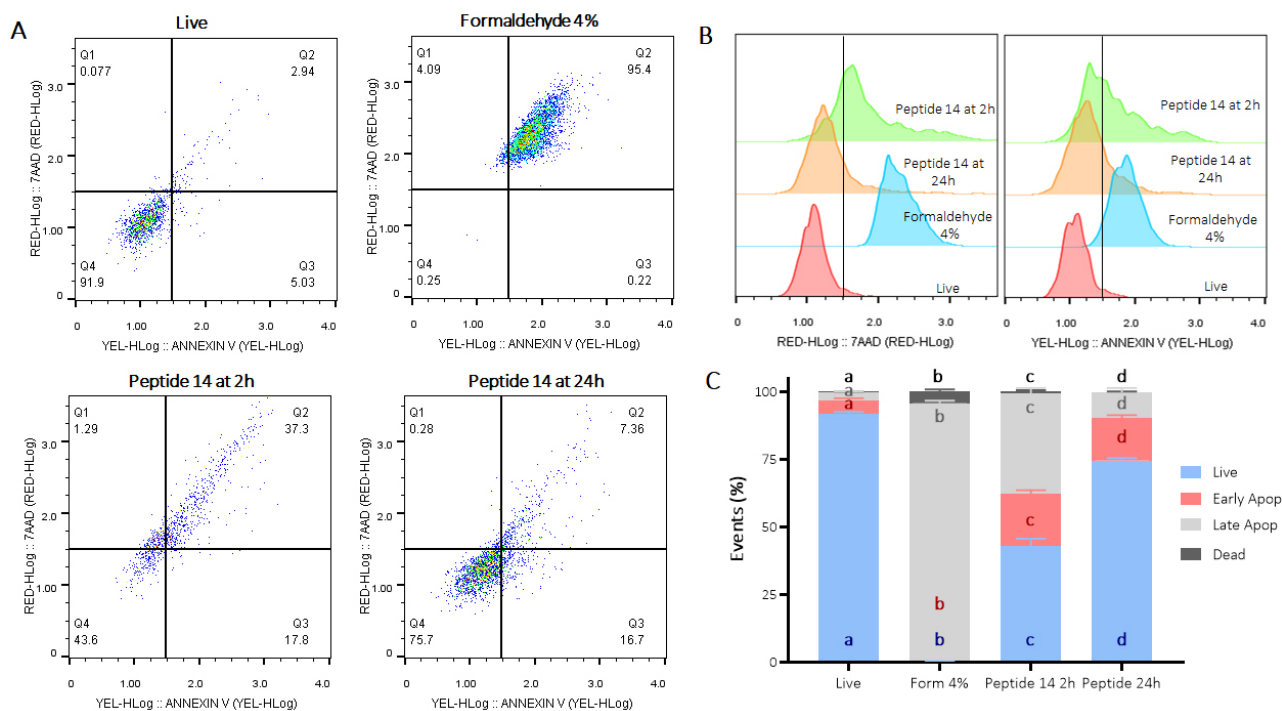


Figure 2. Flow cytometry assay for the determination of apoptosis/necrosis in MCF-7 cells treated for 2 and 24 h with the IC₅₀ of the peptide 14. (A) Representative dot plots of the treatments in the 7-AAD and annexin V channels. Q1: events in necrosis, Q2: events in late apoptosis, Q3: early apoptosis and Q4: living events. Apoptosis control: formaldehyde 4%, necrosis control: ethanol 50%, negative control: RPMI 1640 medium. (B) Representative histograms of the change in fluorescence of the treatments evaluated. (C) Bar graph of the percentage of events related to live cells, in early, late apoptosis or necrosis in each of the treatments ($n = 3$), two-way ANOVA with Tukey's multiple comparisons. Significant differences between the living (blue), early apoptosis (red), late apoptosis (gray) and dead (black) groups are denoted. For those with the same letter, the difference between the means is not statistically significant. If they have different letters, they are significantly different. Apop: apoptosis; Form: formaldehyde

of the MCF-cells 7 suffers death events due to necrosis/permeabilization of the cell membrane at both times evaluated. In turn, after 2 h of treatment with the peptide 14, there is a significant activation of caspases in 27% of the cell population, of these, 12% are cells still alive while 15% are dead cells, which indicates a greater population in late rather than early apoptosis events, data that correlate with those previously shown in Figure 2. Likewise, 24 h post-treatment with the peptide, significant caspase activation is maintained in 21% of the population; correlating with previous results where apoptotic events are still observed at this time point (Figure 2).

Regarding the depolarization of the mitochondrial membrane, in Figure 4 Panel B it is observed how treatment with peptide 14 for 2 and 24 h generated a decrease in fluorescence in the YEL channel (yellow) indicating a significant mitochondrial depolarization of the treated cells. Such depolarization is characterized in living cells and does not present significant differences at the two times evaluated, indicating that this population of cells is in early apoptosis processes.

To corroborate that the cells have entered into apoptotic processes, Figure 5 shows the change in the relative expression of anti- and pro-apoptotic genes after 2 and 24 h of treatment with the peptide 14. Regarding the anti-apoptotic genes *Bcl-2* and *Survivin*, a trend of decreased expression is evident 2 h post-stimulus, which would induce an increase in cell apoptosis correlated with what is evident in Figure 2. After 24 h its expression is regulated, returning to its basal state, which could be evidence of a response by the cells to avoid the cytotoxic effect.

Regarding pro-apoptotic genes, differences are noted in the response at different times. After 2 h of treatment, a significant increase in the expression of *Caspase 8* was evident, this could indicate that part of the caspase activation (Figure 3) is given by the initiation of the extrinsic apoptosis cascade induced by a mechanism not yet described. Associated to it, Caspase 8 can participate in the activation of the intrinsic pathway through cleavage of Bid that with Bax would promote mitochondrial depolarization. The genes responsible for encoding both proteins are significantly upregulated indicating the need of these molecules

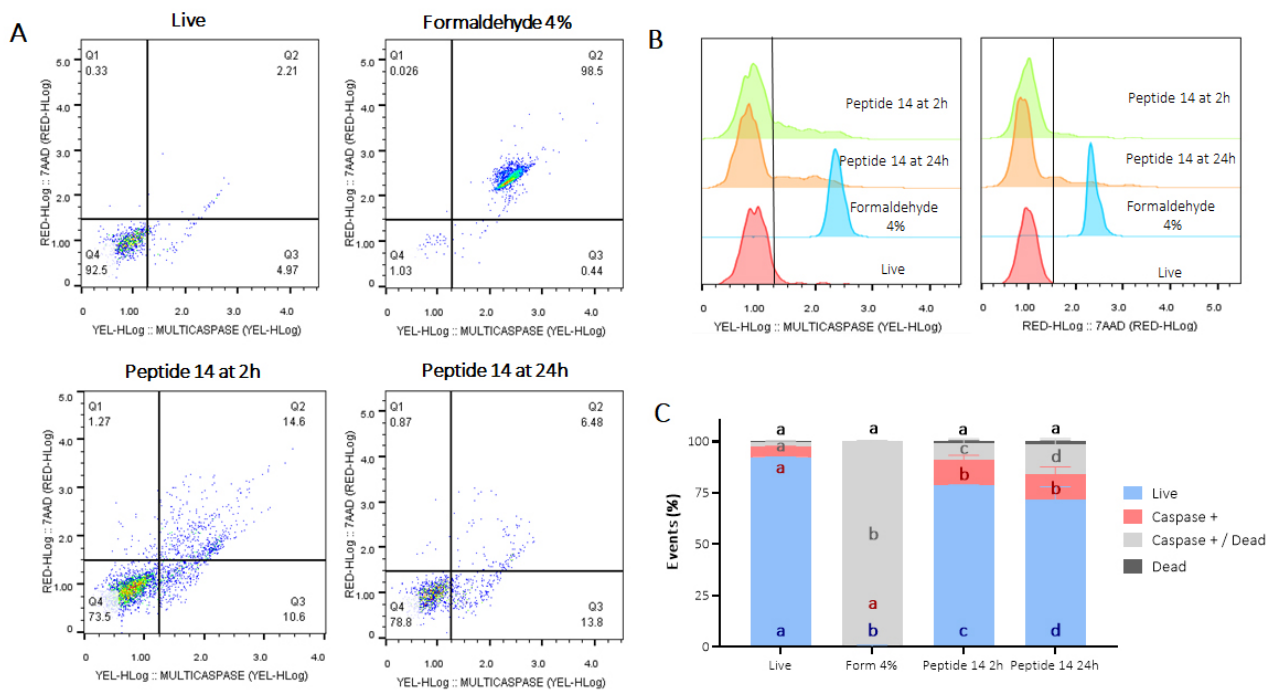


Figure 3. Flow cytometry assay for the determination of caspase activation in MCF-7 cells treated for 2 and 24 h at the IC_{50} concentration of the peptide 14. (A) Representative dot plots of the treatments. Q1: cell death events, Q2: caspase activation events in dead cells, Q3: caspase activation in living cells, and Q4: living events. Apoptosis control: Form (formaldehyde) 4%, and negative control: RPMI 1640 medium. (B) Representative histograms of the change in fluorescence of the treatments evaluated. (C) Bar graph of the percentage of events related to living cells, caspase activation or dead cells in each of the treatments ($n = 3$), two-way ANOVA with Tukey's multiple comparisons. Significant differences between the living (blue), caspase positive (red), caspase positive and dead (gray) and dead (black) groups are denoted. For those with the same letter, the difference between the means is not statistically significant. If they have different letters, they are significantly different

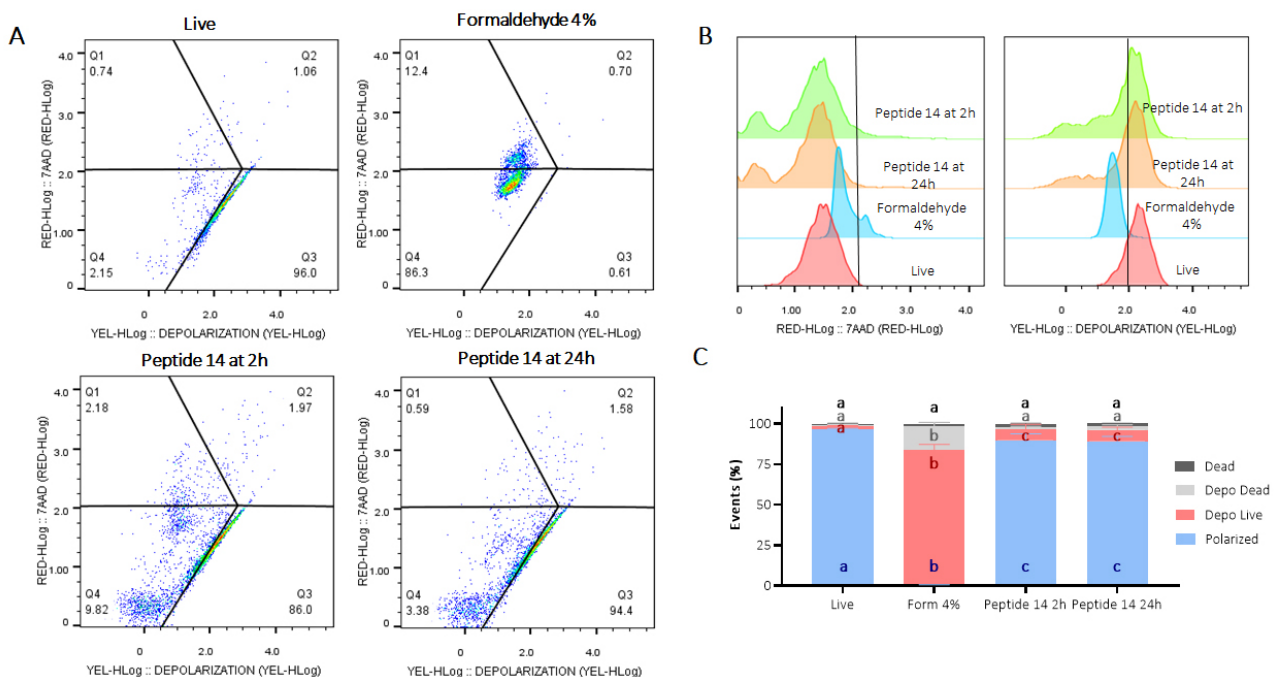


Figure 4. Flow cytometry assay for mitochondrial membrane depolarization in MCF-7 cells treated with peptide 14 at IC_{50} concentration for 2 and 24 h. (A) Representative dot plots of treatments. Q1: cell death events, Q2: mitochondrial depolarization events in dead cells, Q3: mitochondrial depolarization in living cells, Q4: living cells with polarized mitochondria. Apoptosis control: Form (formaldehyde) 4%; negative control: RPMI 1640 medium. (B) Representative histograms showing fluorescence change of evaluated treatments. (C) Bar graph depicting percentage of events related to living polarized cells, cells with depolarized mitochondria, or necrosis in each treatment ($n = 3$). Analysis: two-way ANOVA with Tukey's multiple comparisons. Significant differences between the polarized cells (blue), living cells with depolarized mitochondria (red), dead cells with depolarized mitochondria (gray) and dead (black) groups are denoted. For those with the same letter, the difference between the means is not statistically significant. If they have different letters, they are significantly different

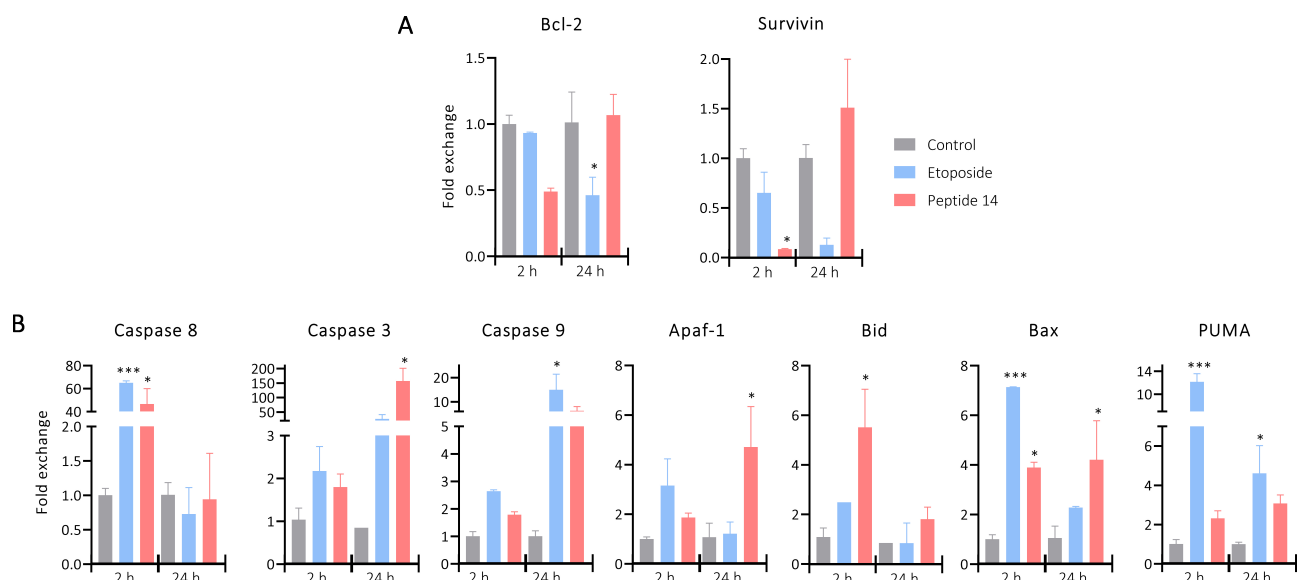


Figure 5. Bar plot of the change in the relative expression of (A) anti-apoptotic and (B) pro-apoptotic genes in MCF-7 cells treated for 2 and 24 h with the IC_{50} of the peptide 14 ($n = 2$). One-way ANOVA with Tukey multiple comparisons (* $p < 0.05$, ** $p < 0.01$ and *** $p < 0.001$) related to control at each time point. Positive control: cells with medium and negative control: etoposide 150 μ M

to continue with the apoptotic process, which would lead to the release of Apaf-1 that together with Caspase 9 would form the apoptosome and involve also the activation of Caspase 3.

After 24 h of treatment with the peptide 14, Caspase 8 returns to its basal expression, probably because the peptide is no longer found in the culture medium to keep this pathway active. While *Caspase 3* presents a significant increase in its expression correlated with the tendency to increase in *Bid* and *Caspase 9* and the significant increase in *Bax* and *Apaf-1*. This could be a response to the initial effect of the peptide that, as a secondary pathway, induced the intrinsic apoptosis pathway and thus prolonged its effect.

Figure 6 Panel A shows how after treatment at 2 and 24 h with the peptide 14, an increase in fluorescence is generated, which indicates an increase in the production of reactive oxygen species by the cells. In Panel B it is evident that the peptide induces significant activation of reactive oxygen species, 2 h post-treatment 24% of the population increases reactive oxygen species production and 24 h later 17% of the population is still positive.

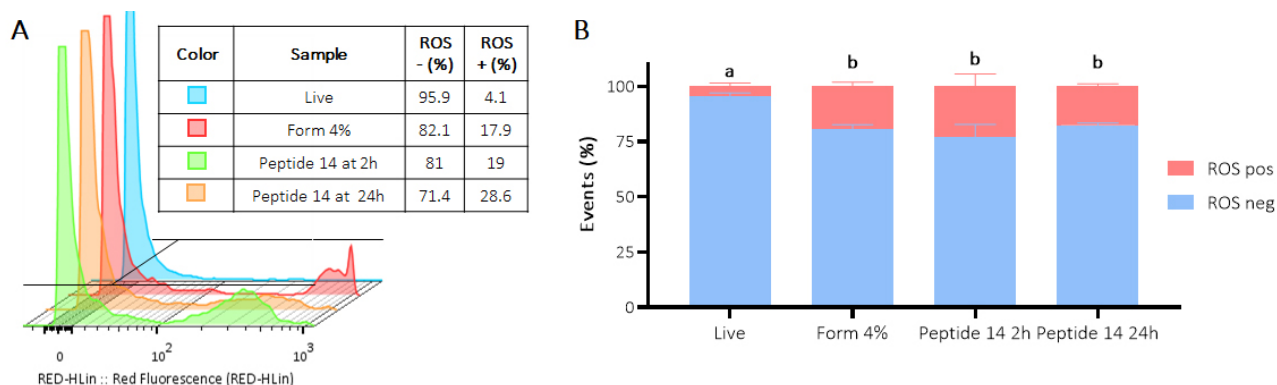


Figure 6. Flow cytometry assay for the determination of the presence of reactive oxygen species (ROS) in MCF-7 cells treated for 2 and 24 h with the IC_{50} of the peptide 14. (A) Representative histograms of the change in fluorescence of the treatments evaluated. Positive control: Form (formaldehyde) 4%, and negative control: RPMI 1640 medium. (B) Bar graph of the percentage of events with ROS production in each of the treatments ($n = 3$), two-way ANOVA with Tukey's multiple comparisons. Significant differences between the negative ROS release (blue) and positive ROS release (red) groups are denoted. For those with the same letter, the difference between the means is not statistically significant. If they have different letters, they are significantly different

To determine other effects associated with the cytotoxic effect induced by peptide 14, the wound-healing test was carried out. **Figure 7** Panels A and B show that after 12 h in the cells without treatment (control), there is a significant wound closure in 10%, and at 24 h this closure was 15%. With the positive control, it was observed that wound closure was significant at 12 h with 15% and at 24 h the wound had closed at 20%. Contrary to these results, after 12 and 24 h of treatment with the peptide 14 the wound area decreased by 1% and 2%, respectively, which is not significantly different from the negative control, indicating that the peptide decreases collective cell migration.

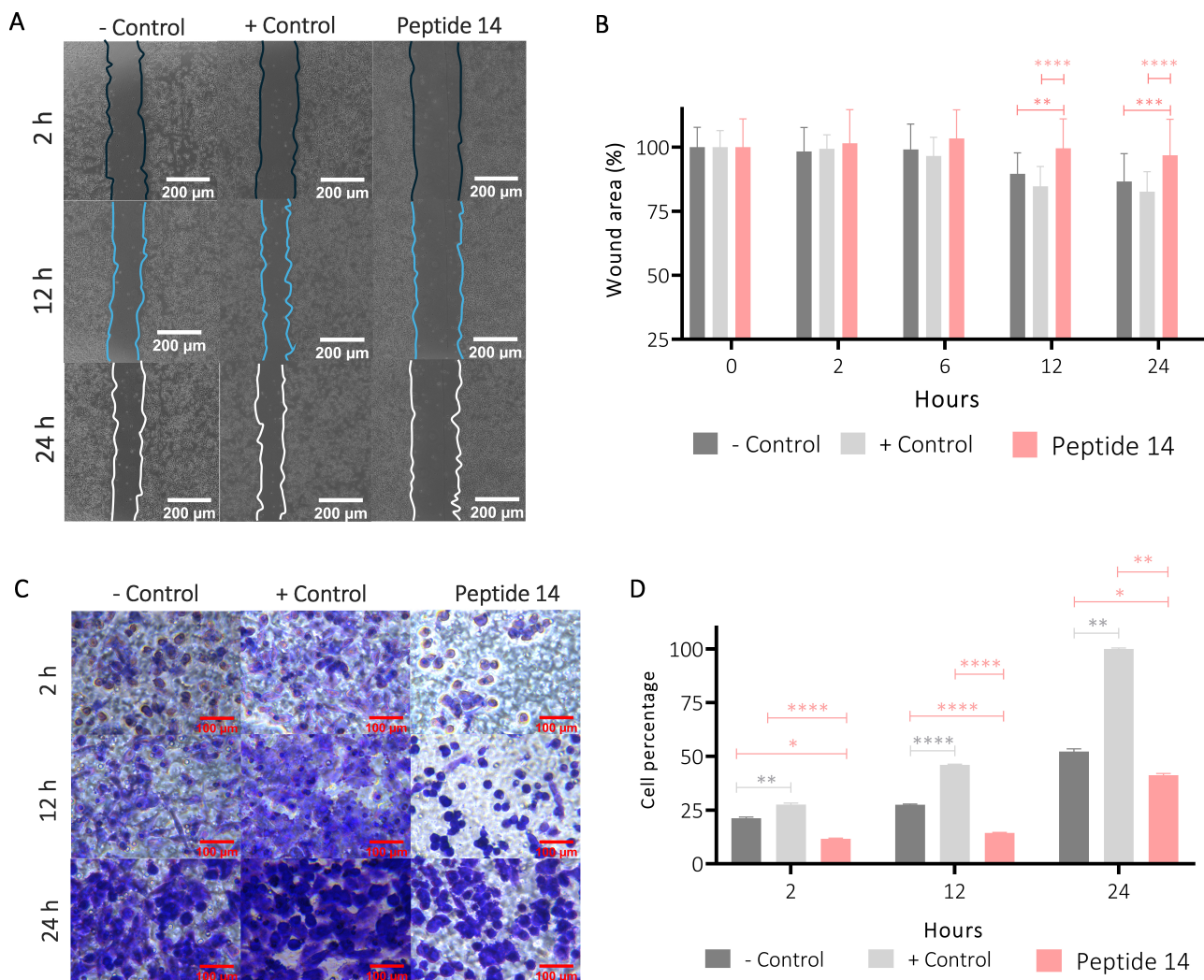


Figure 7. Effect of the IC_{50} of the peptide 14 on MCF-7 cell migration. (A) Representative 20 \times photomicrographs of the wound area after 2, 12 and 24 h of treatment. (B) Bar graph of % wound area after 2, 6, 12 and 24 h of treatment ($n = 2$). (C) Representative 40 \times photomicrographs of the transwell membrane with migrating cells after 2, 12 and 24 h of treatment ($n = 2$). (D) Bar graph of the relative percentage of cells on the membrane after 2, 12 and 24 h of treatment based on crystal violet absorbance at 570 nm ($n = 2$). One-way ANOVA with Tukey's multiple comparisons. * $p < 0.05$, ** $p < 0.01$, *** $p < 0.001$ and **** $p < 0.0001$ related to control at each time point. Positive control: cells with RPMI 1640 medium supplemented with 20% FBS, negative control: cells with RPMI 1640 medium supplemented with 5% FBS

This effect on migration was corroborated by a transwell migration assay (**Figure 7** Panels C and D), where it was shown that from 2 h of treatment of the cells with the peptide 14 and up to 24 h later, the migratory capacity of the cells decreased significantly when compared with that of the basal state (control) or against the positive migration control (medium with 20% FBS).

Figure 8 shows the effect of peptide 14 on the invasion of MCF-7 cells after 24 h of treatment. In Panel A it is evident that the peptide significantly reduces cell invasion and in Panel B we corroborate this information with the count of cells per visual field that are crossing the membrane showing that this peptide can diminish the ability of the cells to become motile and to navigate through the extracellular

matrix. In order to determine if this effect on invasion was mediated by the proteolytic activity of matrix metalloproteases (MMPs), more specifically MMP2 and MMP9, the zymography presented in Figure 8 (Panels C and D) was performed, where it is observed that there is no decrease in pro-MMP2 activity when the cells were treated for 24 h with the peptide 14. On the other hand, a decrease in pro-MMP9 was observed, which could be related to the lower invasive capacity of the cell.

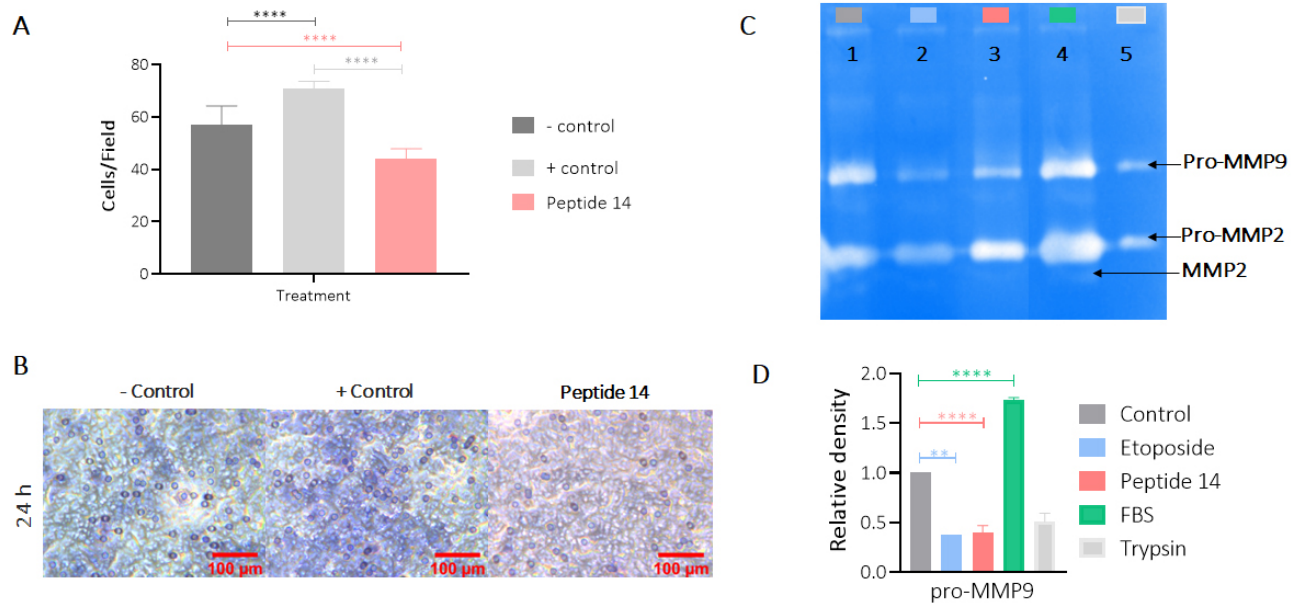


Figure 8. Effect of the IC_{50} of peptide 14 on the invasion of MCF-7 cells after 24 h of treatment. (A) Bar graph of the percentage of cells on the membrane after 24 h of treatment. One-way ANOVA with Tukey's multiple comparisons. * $p < 0.05$, ** $p < 0.01$, *** $p < 0.001$ and **** $p < 0.0001$ related to control group ($n = 2$). (B) Representative 40 \times photomicrographs of the membrane with migrating cells after 24 h of treatment. Positive control: cells with RPMI 1640 medium supplemented with 20% FBS and negative control: cells with RPMI 1640 medium supplemented with 5% FBS ($n = 2$). (C) Gelatinase zymography. Lane 1: control (RPMI 1640 medium FBS 5%), 2: etoposide 150 μ M, 3: peptide 14 at IC_{50} , 4: FBS and 5: trypsin D. Graphic representation of the relative activity of gelatinase MMP9. One-way ANOVA with Tukey's multiple comparisons. * $p < 0.05$, ** $p < 0.01$, *** $p < 0.001$ and **** $p < 0.0001$ related to control group ($n = 2$)

To evaluate if the peptide 14 would also have an immunomodulatory activity the cytokine release profile of MCF-7 cells was assessed. Figure 9 shows the change in the release of cytokines induced by treatment with peptide for 2 and 24 h. A significant decrease in the expression of IL-6 and IL-10 can be seen, as well as a downregulation of arginase. The other cytokines evaluated did not have any significant changes or patterns between treatment and not treated cells. The decrease in the release of these 3 cytokines suggests that the peptide 14 maintains part of the immunomodulatory capacity that had been reported by the whole lactoferrin protein.

The results obtained here allowed us to determine that the peptide 14 induces in MCF-7 cells the decrease in cell viability associated with apoptotic events, these events occur due to the activation of both the intrinsic and extrinsic pathways of the apoptosis. The activation of caspases, the overexpression of pro-apoptotic genes and the release of reactive oxygen species characterized this programmed cell death. Furthermore, it was evidenced that the peptide exerts, as an associated mechanism, the decrease in the collective and single migration capacities of the cells; and the cell invasion capacity related to the decrease in MMP9 activity. In turn, it induced a significant decrease in the expression of IL-6, IL-10 and arginase; cytokines involved in migration and invasion processes.

To evaluate the toxicity that the peptide 14 exerts in a living organism with an innate immune system at physiological temperature. The *Galleria mellonella* larvae were inoculated with the peptide at a concentration of 800 μ g/mL, corresponding to 30 times the IC_{50} value determined in the MTT assays for the MCF-7 cell line. The survival of each of the individuals was monitored daily for 10 days (Figure 10), showing that at the concentration evaluated the survival was 90% or higher during this period; therefore, it was not possible to determine the lethal dose 50 (LD_{50}) under the test conditions. The dose evaluated in

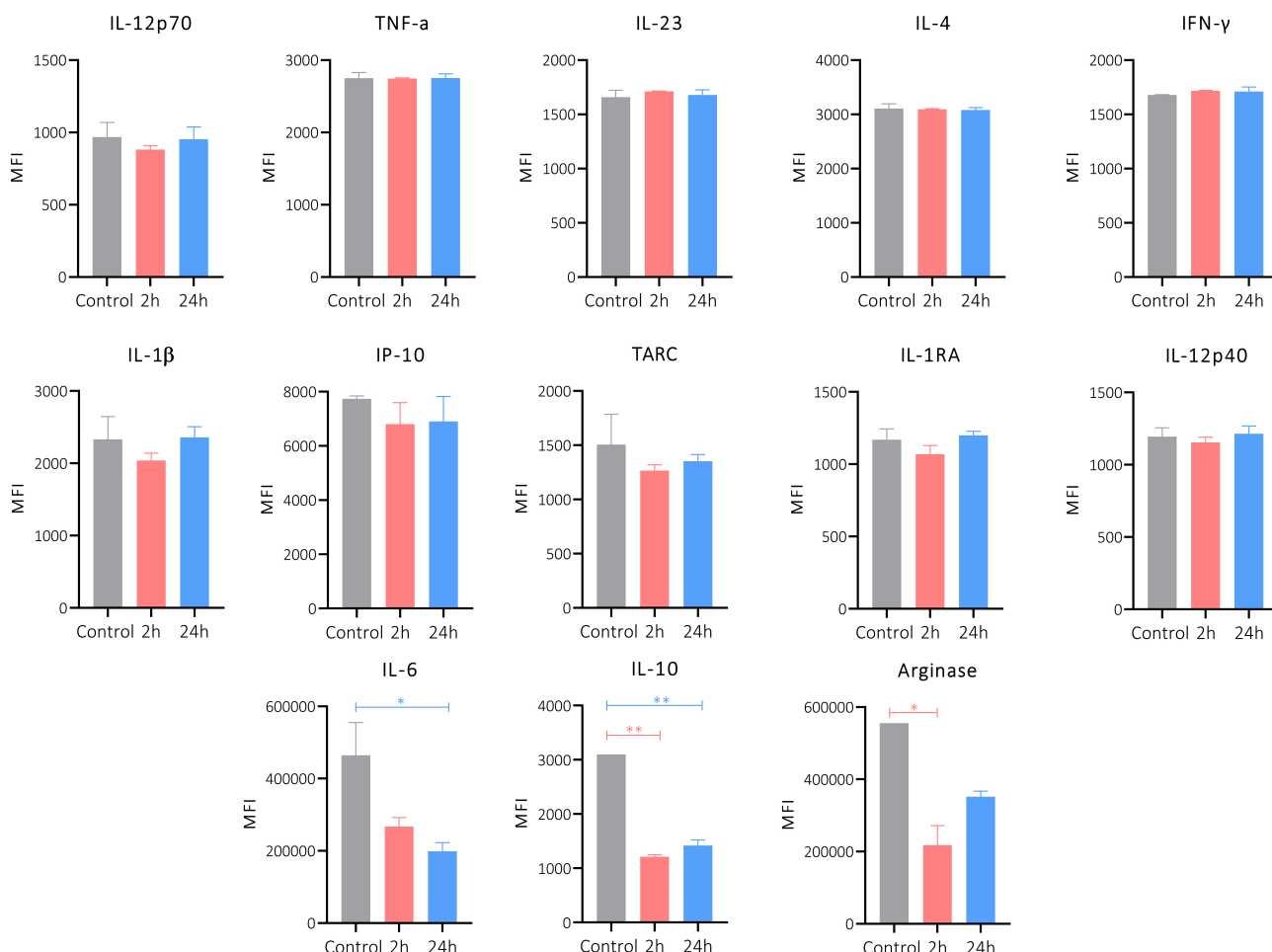


Figure 9. Cytokine release profile of MCF-7 cells treated for 2 and 24 h with the peptide 14 at the IC_{50} concentration. Bar graph of the change in mean fluorescence intensity by the LEGENDplex kit. One-way ANOVA with Tukey's multiple comparisons. * $p < 0.05$, ** $p < 0.01$, *** $p < 0.001$ and **** $p < 0.0001$ related to control group. Control: cells with RPMI 1640 medium supplemented with 5% FBS ($n = 2$)

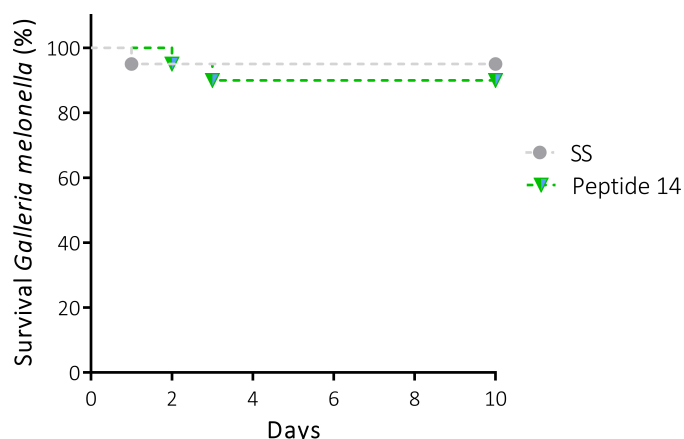


Figure 10. Survival curve (Kaplan Meier) of *Galleria mellonella* larvae treated with the peptide 14 at 40 mg/kg reconstituted in saline solution (SS) ($n = 10$, with two biological replicates)

this model was 40 mg/kg, which indicates that the LD_{50} is above this value, classifying the peptide as moderately toxic. Considering that there was no mortality greater than one larva per trial, it is important to highlight that the peptide does not induce acute cytotoxicity in this model, nor an exacerbated immune response.

Discussion

The palindromic sequence RWQWRWQWR ($1R^5R^9R$) was designed from sequence RRWQWR. This peptide has shown antibacterial activity in Gram-positive and Gram-negative strains, as well as anticancer activity

in breast and colon cancer cells. The action mechanism proposed for LfcinB in bacteria is based in an initial electrostatic interaction between the positively charged side chain (Arg) and the molecules negatively charged in bacterial surface. This interaction allows that the side chain of Trp interact with the lipid layer of membrane, inducing membrane disruption and/or internalization of the peptide to act in target in cytoplasm or nucleus [8, 9]. In a similar way, LfcinB interacts with the molecules negatively charged on cancer cell surface due to the impaired phospholipid in the external cell membrane and a higher expression of O-glycosylated mucins. The electrostatic interaction between the peptide and cell surface could be unspecific allowing that the peptide interact selectively with cancer cells.

Here in, we have found that when a D-amino acid independently of the residue (Arg, Trp or Gln) and/or its position in the sequence changed one L-amino acid, the cytotoxic effect in MCF-7 cells decreased significantly. When the L-Arg was replaced by D-Arg, the net charge of the peptide was not modified. In similar way when the respectively L-amino acid was changed by D-Trp or D-Gln the hydrophobicity or polarity was unmodified. The change of any L-amino acid by its D-amino acid did not affect the net charge, polarity, and hydrophobicity, only changed one chiral center. Added, when ^{1,5,9}L-Arg, ^{3,7}L-Gln or ^{2,4,6,8}L-Trp were changed simultaneously by the respective D-amino acids their net charge, polarity and hydrophobicity were not affected, only three, two or four chiral centers were modified, respectively. In these cases, the cytotoxic effect on MCF-7 cells was also lost. These results suggested that the interaction cell-peptide involved in the cytotoxic effect could be related with an electrostatic interaction that is unspecific and allows the peptide reach the cell surface and, another interaction, similar to receptor-ligand which could be specific and require interaction between the side chain of the L-amino acid of peptide and sidechains of L-amino acids of the receptor.

Besides that, functionalization with the RGD motif in the N-terminal exerts a greater cytotoxic effect in all breast cancer cell lines evaluated suggesting it has an effect on different molecular subtypes, even though the response differed among them. Lines BT-474 and MDA-MB-231 were less sensitive to treatment. In the case of the luminal B subtype, functionalization with the tripeptide, although it maintained the cytotoxicity of the palindrome, did not significantly increase it. This could be due to the fact that this cell line expresses the $\alpha\beta3$ integrin to a lesser extent [19], the effect being related to the sequence derived of LfcinB more than with the guide tripeptide.

In the MDA-MB-468 and MCF-7 cells treated with peptide 14, an increase in the cytotoxic effect was evident compared those treated with peptide ¹R⁵R⁹, generating a cytotoxic effect at lower concentrations of the peptide and without significant variations at the three times evaluated, determining that the peptide 14 exerts a rapid and long-lasting cytotoxic effect. Both lines overexpress the $\alpha\beta3$ integrin [19, 20] suggesting that the recognition of the RGD tripeptide by this receptor favours the cytotoxic effect of the peptide 14.

As a control, a primary culture of fibroblasts extracted from the foreskin of a newborn was chosen. These cells have a higher expression of the $\alpha\beta3$ integrin, allowing us to identify the effect of the addition of the RGD motif on non-cancerous cells. It was evident that after 2 h there of treatment is a decrease in cellular metabolism that reduces its viability by 50%, however, after 24 h this effect on cellular metabolism is minor since viability was close to 80% and finally, 48 h after treatment with the peptide, the cells have recovered their normal activity. This suggests an initial effect similar to that of cancer cells, the peptide fails to induce death in fibroblasts, only to decrease their metabolism.

The type of death exerted by the peptide 14 was evaluated in MCF-7, showing that it mostly induces an apoptotic event associated with the activation of caspases and depolarization of the mitochondrial membrane. Both processes have been previously observed in other cell lines, such as Jurkat derived from leukaemia, treated with LfcinB, which after 2 h of treatment with 200 $\mu\text{g}/\text{mL}$ of this 25 amino acid peptide induced apoptosis in 80% of the cell population, generating caspase activation in only 20% [21, 22]. The 13-residue, peptide 14, at the same treatment time (2 h) but at a 7-fold lower concentration, induced similar effects in the breast cancer-derived MCF-7 cell line. Furthermore, it has been reported that other short peptides derived from LfcinB that contain the minimal motif have also induced cell death by apoptosis in

other cell lines derived from oral cancer, colon cancer and breast cancer, suggesting that peptides derived from LfcinB induce cell death by apoptosis in a similar manner to LfcinB.

In addition, the overexpression of *Caspase 8*, *Bid*, *Bax* at 2 h of treatment and of *Apaf-1*, *Caspase 9* and *3* at 24 h of treatment was characterized, confirming the apoptotic process. Changes in the relative expression of genes at short times have been characterized in other cell types under pro-apoptotic stimuli. It has been shown that the transcription of genes involved in apoptosis begins from 1 h post-stimulus, and even some genes such as *PUMA* present a peak increase in relative expression at 2.5 h that decreases at later times [23]. In MCF-7 changes in the expression of *Bax* and *Bcl-2* have been determined from 6 to 24 h post-stimulus [24].

The activation of Caspase 8 and Caspase 9 indicates that the peptide 14 causes the activation of both apoptotic pathways. This dual process was evidenced by flow cytometry in MCF-7 cells treated with the dimeric peptide (RRWQWR-Nal-KKLG)₂-K-Ahx derivative of LfcinB [25] and in Jurkat cells by western-blot when treated with LfcinB [21]. These results reinforce the hypothesis that peptides derived from LfcinB that contain the minimal activity motif share mechanism(s) of action that involve both the intrinsic and extrinsic pathways of apoptosis to exert their cytotoxic effect. In addition, it correlates with our results on D-amino acid modifications, where a possible specific interaction is needed to activate the apoptotic extrinsic pathway, this item needs to be studied in depth to fully unveil the mechanism of action of the peptide 14.

The results on cell migration and invasion are of great interest since in previous reports LfcinB has not generated a decrease in invasion processes in MCF-7 [26]. Our results suggest that peptide 14 derived from the palindrome, possibly also induces other mechanisms of action associated with the cytotoxic effect different from those described for LfcinB.

Considering that LFB, the protein from which this synthetic peptide is derived, is characterized by having an immunomodulatory effect, we evaluated whether this peptide would retain it. Here we reported a decrease in IL-6, IL-10 and arginase related to peptide 14, which correlates with a decrease in migration and invasion. Decreases in IL-6 expression have been reported in in vivo assays in which mice with induced mammary tumours were treated with LFB nanoparticles [27], suggesting that both this 13-residue peptide and the complete protein exert immunomodulatory effects on this cytokine. In a similar way to what was seen with the peptide 14; in A549 cells derived from lung cancer, it has been observed that in both in vivo and in vitro assays, treating them with LFB induces a decrease in expression of these cytokines related to the inhibition of tumour growth [28].

The decrease in the release of these cytokines and arginase suggests that the peptide 14 maintains part of the immunomodulatory capacity that has been previously described for the protein, at least against cancer-derived cells. This is in line with what is evidenced in cells derived from colon cancer and leukaemia, where peptides containing the minimal activity motif can exert a cytotoxic effect through more than one mechanism of action [28–30] and it is necessary to evaluate this topic in greater depth.

In conclusion, peptide 14 induces death in MCF-7 cells, which does not significantly compromise the cell membrane but rather triggers cellular apoptotic events by activation of both the intrinsic and extrinsic pathways. This was evidenced by a significant increase in the transcript of Caspase 8 and 9 together with other pro-apoptotic genes, the activation of these caspases by flow cytometry, the depolarization of the mitochondrial membrane, and the release of reactive oxygen species. In turn, it was observed that the peptide decreases the migration and invasion capacity of cells and the release of interleukins associated with the autoregulated signalling of these processes.

These results suggest that peptide 14 can be considered a promising molecule for the future development of an anticancer therapy based on peptide sequences.

Abbreviations

ER: oestrogen receptor

HER2: human epidermal growth factor receptor 2

LfcinB: lactoferricin B

MMPs: matrix metalloproteases

PR: progesterone receptor

t_R : retention time

Supplementary materials

The supplementary figures for this article are available at: https://www.explorationpub.com/uploads/Article/file/100852_sup_1.pdf.

Declarations

Author contributions

ABC: Conceptualization, Software, Validation, Formal analysis, Investigation, Data curation, Writing—original draft. DCA: Validation, Formal analysis, Investigation, Data curation. YVC: Validation, Formal analysis, Investigation. CPG: Conceptualization, Project administration, Funding acquisition, Resources. AUP and JLM: Conceptualization, Methodology, Data curation, Supervision, Resources. ZRM: Conceptualization, Resources, Supervision, Writing—review & editing, Project administration, Funding acquisition, Resources. JGC: Conceptualization, Resources, Supervision, Writing—original draft, Writing—review & editing, Project administration, Funding acquisition, Resources. All authors read and approved the submitted version.

Conflicts of interest

The authors declare that they have no conflicts of interest.

Ethical approval

All the experiments were carried out in compliance with the guidelines and standards of Resolution 08430 of 1993 of the Colombian Ministry of Health and Law 84 of 27 December 1989 and were governed by the principles and standards for the care and use of animals, decreed by the institutional Ethics Committee from Science Faculty (Act 03-2018) of the National University of Colombia.

Consent to participate

Not applicable.

Consent to publication

Not applicable.

Availability of data and materials

The raw data supporting the conclusions of this manuscript will be made available by the authors, without undue reservation, to any qualified researcher.

Funding

This research was funded by COLCIENCIAS grant number [RC No. 706-2018]. Project: “Desarrollo de un medicamento contra el cáncer de mama basado en un péptido polivalente derivado de la LfcinB: Estudio de la fase preclínica (fase cero), caracterización fisicoquímica de un lote del fármaco para estudios preclínicos”. Code [110180762973]. The funders had no role in study design, data collection and analysis, decision to publish, or preparation of the manuscript.

Copyright

© The Author(s) 2024.

References

1. Ferlay J, Colombet M, Soerjomataram I, Parkin DM, Piñeros M, Znaor A, et al. Cancer statistics for the year 2020: An overview. *Int J Cancer*. 2021;149:778–89. [DOI]
2. Testa U, Castelli G, Pelosi E. Breast Cancer: A Molecularly Heterogenous Disease Needing Subtype-Specific Treatments. *Med Sci (Basel)*. 2020;8:18. [DOI] [PubMed] [PMC]
3. Onkar SS, Carleton NM, Lucas PC, Bruno TC, Lee AV, Vignali DAA, et al. The Great Immune Escape: Understanding the Divergent Immune Response in Breast Cancer Subtypes. *Cancer Discov*. 2023;13:23–40. [DOI] [PubMed] [PMC]
4. Johnson KS, Conant EF, Soo MS. Molecular Subtypes of Breast Cancer: A Review for Breast Radiologists. *J Breast Imaging*. 2021;3:12–24. [DOI] [PubMed]
5. Burguin A, Diorio C, Durocher F. Breast Cancer Treatments: Updates and New Challenges. *J Pers Med*. 2021;11:808. [DOI] [PubMed] [PMC]
6. Kc M, Fan J, Hyslop T, Hassan S, Cecchini M, Wang S, et al. Relative Burden of Cancer and Noncancer Mortality Among Long-Term Survivors of Breast, Prostate, and Colorectal Cancer in the US. *JAMA Netw Open*. 2023;6:e2323115. [DOI] [PubMed] [PMC]
7. Xie M, Liu D, Yang Y. Anti-cancer peptides: classification, mechanism of action, reconstruction and modification. *Open Biol*. 2020;10:200004. [DOI] [PubMed] [PMC]
8. Kordi M, Borzouyi Z, Chitsaz S, Asmaei MH, Salami R, Tabarzad M. Antimicrobial peptides with anticancer activity: Today status, trends and their computational design. *Arch Biochem Biophys*. 2023;733:109484. [DOI] [PubMed]
9. Zhang Y, Lima CF, Rodrigues LR. Anticancer effects of lactoferrin: underlying mechanisms and future trends in cancer therapy. *Nutr Rev*. 2014;72:763–73. [DOI] [PubMed]
10. Richardson A, de Antueno R, Duncan R, Hoskin DW. Intracellular delivery of bovine lactoferricin's antimicrobial core (RRWQWR) kills T-leukemia cells. *Biochem Biophys Res Commun*. 2009;388:736–41. [DOI] [PubMed]
11. Barragán-Cárdenas AC, Insuasty-Cepeda DS, Vargas-Casanova Y, López-Meza JE, Parra-Giraldo CM, Fierro-Medina R, et al. Changes in Length and Positive Charge of Palindromic Sequence RWQWRWQWR Enhance Cytotoxic Activity against Breast Cancer Cell Lines. *ACS Omega*. 2023;8:2712–22. [DOI] [PubMed] [PMC]
12. Li L, Chen X, Yu J, Yuan S. Preliminary Clinical Application of RGD-Containing Peptides as PET Radiotracers for Imaging Tumors. *Front Oncol*. 2022;12:837952. [DOI] [PubMed] [PMC]
13. Insuasty-Cepeda DS, Barragán-Cárdenas AC, Ochoa-Zarzosa A, López-Meza JE, Fierro-Medina R, García-Castañeda JE, et al. Peptides Derived from (RRWQWRM₂K₂)-K-Ahx Induce Selective Cellular Death in Breast Cancer Cell Lines through Apoptotic Pathway. *Int J Mol Sci*. 2020;21:4550. [DOI] [PubMed] [PMC]
14. Lara-Márquez M, Báez-Magaña M, Raymundo-Ramos C, Spagnuolo PA, Macías-Rodríguez L, Salgado-Garciglia R, et al. Lipid-rich extract from Mexican avocado (*Persea americana* var. *drymifolia*) induces apoptosis and modulates the inflammatory response in Caco-2 human colon cancer cells. *J Funct Foods*. 2020;64:103658. [DOI]
15. Luminex LTG [Internet]. Diasorin; [cited 2019 Oct 29]. Available from: <https://us.diasorin.com/en/luminex-ltg>
16. LEGENDplex™ Human Macrophage/Microglia Panel [Internet]. BioLegend; [cited 2023 Dec 1]. Available from: https://www.biolegend.com/Files/Images/media_assets/pro_detail/datasheets/75062_Hu_Macrophage-Microglia_Panel_V01.pdf

17. Sandoval-Usme MC, Umaña-Pérez A, Guerra B, Hernández-Perera O, García-Castellano JM, Fernández-Pérez L, et al. Simvastatin impairs growth hormone-activated signal transducer and activator of transcription (STAT) signaling pathway in UMR-106 osteosarcoma cells. *PLoS One*. 2014;9:e87769. [DOI] [PubMed] [PMC]
18. Cabezas-Perez RJ, Vallejo-Pulido AF, Freyre-Bernal SI, Umana-Perez A, Sanchez-Gomez M. IGF-II y la gonadotropina corionica regulan la proliferacion, migracion e invasion de celulas de trofoblasto humano. *Acta Biol Colomb*. 2011;16:143–52. Spanish.
19. ITGAV [Internet]. The Human Protein Atlas; [cited 2023 Dec 2]. Available from: <https://www.proteinatlas.org/ENSG00000138448-ITGAV/cell+line>
20. Gai Y, Jiang Y, Long Y, Sun L, Liu Q, Qin C, et al. Evaluation of an Integrin $\alpha_v\beta_3$ and Aminopeptidase N Dual-Receptor Targeting Tracer for Breast Cancer Imaging. *Mol Pharm*. 2020;17:349–58. [DOI] [PubMed] [PMC]
21. Mader JS, Salsman J, Conrad DM, Hoskin DW. Bovine lactoferricin selectively induces apoptosis in human leukemia and carcinoma cell lines. *Mol Cancer Ther*. 2005;4:612–24. [DOI] [PubMed]
22. Mader JS, Richardson A, Salsman J, Top D, de Antueno R, Duncan R, et al. Bovine lactoferricin causes apoptosis in Jurkat T-leukemia cells by sequential permeabilization of the cell membrane and targeting of mitochondria. *Exp Cell Res*. 2007;313:2634–50. [DOI] [PubMed]
23. Fester N, Zielonka E, Goldmann J, Frombach A, Müller-Kuller U, Gutfreund N, et al. Enhanced pro-apoptosis gene signature following the activation of TAp63 α in oocytes upon γ irradiation. *Cell Death Dis*. 2022;13:204. [DOI] [PubMed] [PMC]
24. Thomadaki H, Talieri M, Scorilas A. Treatment of MCF-7 cells with taxol and etoposide induces distinct alterations in the expression of apoptosis-related genes *BCL2*, *BCL2L12*, *BAX*, *CASPASE-9* and *FAS*. *Biol Chem*. 2006;387:1081–6. [DOI] [PubMed]
25. Insuasty-Cepeda DS, Barragán-Cárdenas AC, Ardila-Chantre N, Cárdenas-Martínez KJ, Rincón-Quiñones I, Vargas-Casanova Y, et al. Non-natural amino acids into LfcinB-derived peptides: effect in their (i) proteolytic degradation and (ii) cytotoxic activity against cancer cells. *R Soc Open Sci*. 2023;10:221493. [DOI] [PubMed] [PMC]
26. Rahman R, Fonseka AD, Sua S, Ahmad M, Rajendran R, Ambu S, et al. Inhibition of breast cancer xenografts in a mouse model and the induction of apoptosis in multiple breast cancer cell lines by lactoferricin B peptide. *J Cell Mol Med*. 2021;25:7181–9. [DOI] [PubMed] [PMC]
27. El-Fakharany EM, Ashry M, Abd-Elaleem AH, Romeih MH, Morsy FA, Shaban RA, et al. Therapeutic efficacy of Nano-formulation of lactoperoxidase and lactoferrin via promoting immunomodulatory and apoptotic effects. *Int J Biol Macromol*. 2022;220:43–55. [DOI] [PubMed]
28. Cutone A, Rosa L, Ianiro G, Lepanto MS, Bonaccorsi di Patti MC, Valenti P, et al. Lactoferrin's Anti-Cancer Properties: Safety, Selectivity, and Wide Range of Action. *Biomolecules*. 2020;10:456. [DOI] [PubMed] [PMC]
29. Pan W, Chen P, Chen YS, Hsu H, Lin C, Chen W. Bovine lactoferricin B induces apoptosis of human gastric cancer cell line AGS by inhibition of autophagy at a late stage. *J Dairy Sci*. 2013;96:7511–20. [DOI] [PubMed]
30. Furlong SJ, Mader JS, Hoskin DW. Bovine lactoferricin induces caspase-independent apoptosis in human B-lymphoma cells and extends the survival of immune-deficient mice bearing B-lymphoma xenografts. *Exp Mol Pathol*. 2010;88:371–5. [DOI] [PubMed]